ANS MC2015 - Joint International Conference on Mathematics and Computation (M&C), Supercomputing in Nuclear Applications (SNA) and the Monte Carlo (MC) Method • Nashville, TN • April 19-23, 2015, on CD-ROM, American Nuclear Society, LaGrange Park, IL (2015)

ACCELERATION OF SHUTDOWN DOSE RATE MONTE CARLO CALCULATIONS USING THE MULTI-STEP CADIS HYBRID METHOD

Ahmad M. Ibrahim, Douglas E. Peplow, and Robert E. Grove*
Oak Ridge National Laboratory
P.O. Box 2008, Oak Ridge, TN 37831
ibrahimam@ornl.gov

ABSTRACT

Shutdown dose rate (SDDR) analysis requires (1) a neutron transport calculation to estimate space- and energy-dependent neutron fluxes, (2) an activation calculation to compute the distribution of radionuclide inventories and the associated photon sources, and (3) a photon transport calculation to estimate the final SDDR. In some applications, accurate full-scale Monte Carlo (MC) SDDR simulations are needed for immensely large systems that involve massive amounts of shielding materials with complex geometric arrangements. However, these simulations are impractical because accurate calculation of space- and energy-dependent neutron fluxes in these systems is difficult with the MC method even if global variance reduction techniques are used. This paper describes the Multi-Step Consistent Adjoint Driven Importance Sampling (MS-CADIS) hybrid MC/deterministic methodology that accelerates multi-step MC shielding calculations. MS-CADIS speeds up the SDDR neutron MC calculation using an importance function that represents the neutron importance to the final SDDR. Using a simplified example, preliminary results showed that the MS-CADIS method enhanced the efficiency of the SDDR neutron MC calculation by a factor of 550 compared to standard global variance reduction techniques, and that the efficiency enhancement compared to analog MC is higher than a factor of 10,000.

Key Words: Shutdown dose rate, hybrid Monte Carlo/deterministic transport, multi-step shielding analysis, Multi-Step CADIS

1 INTRODUCTION

Shutdown doses in fission and fusion energy systems result from the decay of neutron-induced activation products in irradiated materials. Accurate assessments of shutdown dose rate (SDDR) are critical to support operation, maintenance, and waste disposal planning and to guide possible design changes of critical components in nuclear energy systems. An SDDR calculation involves three steps:

1. a neutron transport calculation to determine the space- and energy-dependent neutron flux distributions,
2. activation calculations to compute the photon source distribution, and

3. a photon transport calculation for estimating the final SDDR.

In some applications, full-scale SDDR simulations are needed for immensely large systems which include massive amounts of shielding materials with complex geometric arrangements. These simulations require calculating the distribution of radioisotopes throughout the entire system. For example, SDDR assessments are required everywhere inside the biological shield (bioshield) of the ITER experimental facility to evaluate the required waiting period after the shutdown of ITER and to identify the locations for which human accessibility should be prohibited [1]. The bioshield is a large cylindrical concrete structure (~30 m tall and 30 m in diameter) surrounding the very complex tokamak machine. Determining the effects on SDDR of important factors such as the cross talk (interactions) between the different ports of ITER is only possible through full-scale simulations that involve all the complex inner details of the ITER tokamak machine [2]. Even without considering the second and the third computational steps, SDDR calculations are much more challenging than one-step neutronics calculations, such as the calculation of the prompt dose rate during operation, because detailed space- and energy-dependent neutron fluxes are needed to estimate the distribution of the radioisotopes causing the SDDR.

Because discrete-ordinates (S_N) methods provide detailed flux information, they may seem more appropriate than Monte Carlo (MC) methods for SDDR neutron transport calculations; however, the truncation errors of S_N methods can adversely affect the accuracy of SDDR predictions. Furthermore, some of the SDDR analyses involve radiation streaming through very narrow solid angles and very complicated pathways, which represent great difficulty for the S_N methods. The computational requirements of full-scale structured mesh S_N simulations of very large and complicated systems such as ITER, which are on the order of tens of processor-years, are only tractable using world-class supercomputers [3]. Even with such expensive requirements, some important geometric features of these complex systems cannot be exactly represented using structured-mesh S_N codes. Unstructured-mesh S_N simulations have been used to calculate SDDR at the interspaces of the ITER diagnostics ports; however, these calculations required the use of coarse meshes with sizes on the order of tens of centimeters in some regions because of the limited scaling capabilities (up to hundreds of processors) of unstructured mesh S_N codes that were used [4]. These coarse meshes and limited angular resolution cause severe discretization errors that can be evidenced by the appearance of negative space- and energy-dependent neutron fluxes in the S_N solutions [5].

The rigorous 2-step (R2S) computational system involves MC neutron and photon transport calculations coupled with an activation step using a dedicated inventory code and library [6]. Accurate full-scale R2S simulations are impractical for large and geometrically complex problems because the calculation of space- and energy-dependent neutron fluxes everywhere in the structural materials is difficult using the MC method. Biasing the neutron MC calculation using an importance function [7] is not straightforward because of the difficulty of explicitly expressing the response function of the neutron calculation, which depends on the subsequent calculation steps.

We developed the Multi-Step Consistent Adjoint Driven Importance Sampling (MS-CADIS) hybrid MC/deterministic method to speed up the SDDR MC neutron transport calculation using an importance function that represents the neutron importance with respect to the final SDDR. The MS-CADIS method uses the CADIS method to develop consistent source biasing and weight-window (WW) variance reduction parameters that efficiently modify the particle

sampling without introducing the inefficiency and false convergence problems caused by an incompatibility between source and transport biasing. The CADIS method has been successfully used for more than a decade in shielding calculations [8, 9]. However, because the MS-CADIS method focuses on multi-step shielding calculations, such as the R2S calculations of SDDR, it develops an importance function for the initial radiation transport calculation (e.g., the neutron calculations in SDDR simulations) that represents the importance of particles to the final response of the overall simulation. This paper explains the theory and implementation of the MS-CADIS method. A simplified example is used to demonstrate the ability of the MS-CADIS method to provide dramatic enhancement in the efficiency of MC SDDR calculations.

2 THE MULTI-STEP CADIS METHOD

2.1 The Multi-Step CADIS Importance Function

A large number of techniques have been developed to increase the efficiency of MC calculations. These modified sampling techniques alter the MC transport simulation in an attempt to sample more particles in regions of phase-space that contribute to the tally. The importance sampling technique [7] uses an importance function to modify the MC sampling process. The importance function $I(\vec{r},E)$can also be viewed as the exact response of the detector due to a source represented by delta function in energy and space $q(\vec{r},E)=\delta(\vec{r}-\vec{r}_0)\delta(E-E_0)$.[†] Theoretically, if the $I(\vec{r},E)$ is known exactly, the detector response R can be expressed as

$$R=\int_V \int_E I(\vec{r},E)q(\vec{r},E)dVdE, \quad (1)$$

where $q(\vec{r},E)$ is the source distribution function. Equation (1) represents an integral equation describing a hypothetical, absolutely efficient MC process where each simulated particle scores the exactly correct expected value as soon as it is emitted from the source without undergoing any physical events. It is necessary to mention that finding the exact importance function is too much to expect [7]. If the importance function were exactly known, performing the random sampling process would not be needed because it would be easier to calculate the response using integration methods. However, throughout the last two decades, the hybrid MC/deterministic techniques have been very successful in dramatically increasing the efficiency of MC calculations using approximate importance functions [8]. The crux of the MS-CADIS approach is to deterministically calculate an appropriate approximation for the importance function $I(\vec{r},E)$, recognizing that, even for the initial steps in multi-step calculations, the response R in Eq. (1) should be the final response of the overall multi-step analysis, not the response of each step on its own.

For the linear integro-differential neutral particle transport equation, a related adjoint equation can be formulated using the identity,

$$\langle\phi(\vec{r},E),q^+(\vec{r},E)\rangle=\langle\phi^+(\vec{r},E),q(\vec{r},E)\rangle, \quad (2)$$

where $\phi(\vec{r},E)$ is the space- and energy-dependent particle flux, $\phi^+(\vec{r},E)$ is the space- and energy-dependent adjoint flux, $q^+(\vec{r},E)$ is the adjoint source space and energy distribution function, and the angle brackets $\langle\cdot\rangle$ signify integration over all energy and space. This adjoint

[†] For simplicity, all the distributions were assumed to be isotropic, but the derivation can be generalized to include the angular variation in a straightforward way.

identity is valid for an arbitrary adjoint source function [10]. However, if the adjoint source function is carefully chosen so that the left-hand side of Eq. (2) represents the response R in Eq. (1) and if the importance function $I(\vec{r}, E)$ is defined as the exact solution of the adjoint transport equation with that specific choice of the adjoint source function, Eq. (2) will have the same form as Eq. (1).

The SDDR caused by decay photons is defined as

$$SDDR = \langle \sigma_d(\vec{r}, E_p), \phi_p(\vec{r}, E_p) \rangle, \tag{3}$$

where σ_d is the flux-to-dose-rate conversion factor at the position of the detector and ϕ_p is the photon flux. Using Eqs. (2) and (3) and setting the photon adjoint source equal to σ_d leads to the following relationship for the photon transport problem:

$$SDDR = \langle q_p^+(\vec{r}, E_p), \phi_p(\vec{r}, E_p) \rangle = \langle q_p(\vec{r}, E_p), \phi_p^+(\vec{r}, E_p) \rangle. \tag{4}$$

Because the adjoint photon flux, $\phi_p^+(\vec{r}, E_p)$ in Eq. (4) expresses the final SDDR caused by a unit photon source at position $\vec{r}$ and with energy E_p, an approximate deterministic estimate of the photon adjoint flux can be used to speed up the MC photon transport calculation of an SDDR problem.

In SDDR analyses the neutron and photon calculations are separated by an activation calculation. Finding the adjoint source of the SDDR neutron calculation is not as simple as the photon calculation because the SDDR is not directly caused by the neutrons; rather, it is caused by the decay photons of the neutron-activated structural materials. *In the MS-CADIS method, we seek an adjoint neutron source whose inner product satisfies the following relationship for the neutron transport problem:*

$$SDDR = \langle q_n^+(\vec{r}, E_n), \phi_n(\vec{r}, E_n) \rangle = \langle q_n(\vec{r}, E_n), \phi_n^+(\vec{r}, E_n) \rangle, \tag{5}$$

where q_n is the neutron source , ϕ_n is the neutron flux, q_n^+ is the neutron adjoint source, and ϕ_n^+ is the neutron adjoint flux. The right equality in Eq. (5) represents the adjoint identity of the neutron transport problem. The equality of the SDDR and the right hand side of Eq. (5), $SDDR = \langle q_n(\vec{r}, E_n), \phi_n^+(\vec{r}, E_n) \rangle$, will have the same form as Eq. (1) if the importance function $I(\vec{r}, E)$ is defined as the adjoint neutron flux ϕ_n^+. However, this requires a specific definition of the neutron adjoint source function to satisfy the left equality of Eq. (5). Even though it may seem counterintuitive to set the *neutron* adjoint identity to be equal to a *photon* response, this can lead to the development of an importance function that represents the importance of the neutrons to the SDDR representing the final response of the overall simulation. From Eqs. (4) and (5), it is clear that the MS-CADIS adjoint neutron source will satisfy the integral equation,

$$\langle q_n^+(\vec{r}, E_n), \phi_n(\vec{r}, E_n) \rangle = \langle q_p(\vec{r}, E_p), \phi_p^+(\vec{r}, E_p) \rangle. \tag{6}$$

If a relationship between the photon source and the neutron flux can be determined, then an adjoint neutron source whose inner product satisfies Eq. (6) can be found.

The photon source can be calculated using a deterministic neutron transport calculation followed by an activation calculation, but finding the relationship between the photon source and the neutron flux requires considering all the neutron transmutation interactions that affect the radioisotope inventory either by creation or depletion. The exact equation describing the radioisotope inventory as a function of the neutron flux is rather complicated [11]. However, a

simple relationship between the photon source and the neutron flux can be derived using quantities calculated by a deterministic neutron transport calculation followed by an activation calculation.

At the end of a fixed irradiation and decay scenario, the photon source which originates from the decay of different radioisotopes can be represented by

$$q_p(\vec{r}, E_p) = \sum_i m_i(\vec{r}) f_i(E_p), \tag{7}$$

where m_i is the mass of each radioisotope i at the end of the scenario and $f_i(E_p)$ is the spectrum of one mass unit of radioisotope i. If the scenario starts from a clean inventory of stable isotopes and if the flux during irradiation does not change due to the changes in the radioisotopes inventory, $m_i(\vec{r})$ can be expressed as the sum of each mass portion of radioisotope i created due to an interaction x with a stable or an activated isotope and the decay or the depletion of the result of this interaction.

By substituting Eqs. (7) into Eq. (6), and changing the order of integration, it can be shown that the following adjoint source satisfies the integral relationship of Eq. (6),

$$q_n^+(\vec{r}, E_n) = \sum_i \left(\int_{E_p} f_i(E_p) \phi_p^+(\vec{r}, E_p) dE_p \times \sum_x m_{ix}(\vec{r}) \frac{\sigma_{xi}(E_n)}{\sigma_{xi}(\vec{r}) \phi_n^t(\vec{r})} \right). \tag{8}$$

Note that the following expression was used to facilitate the derivation,

$$m_i(\vec{r}) = \sum_x m_{ix}(\vec{r}) \frac{\int_{E_n} \sigma_{xi}(E_n) \phi_n(\vec{r}, E_n) dE_n}{\sigma_{xi}(\vec{r}) \phi_n^t(\vec{r})}, \tag{9}$$

where $m_{ix}(\vec{r})$ is the mass at the end of the scenario of each radioisotope i that was originally created by the interaction x at $\vec{r}$, $\sigma_{xi}(E_n)$ is the energy-dependent microscopic cross section of the interaction x that leads to the creation of the radioisotope i or its precursor, $\phi_n^t(\vec{r})$ is the total flux at location $\vec{r}$, and $\sigma_{xi}(\vec{r})$ is the one-group cross section of $\sigma_{xi}(E_n)$ that uses $\phi_n(\vec{r}, E_n)$ as the collapsing vector. Equation (9) represents the mass conservation formula in Eq. (7) multiplied by the same interaction rate per atom in the numerator and the denominator. If the irradiation scenario starts with an initial radioisotope inventory, this initial inventory should not be considered in the masses calculated in Eq. (9) because it should not affect the space and energy distribution of the neutron adjoint source.

Determining all of the interactions that cause the creation of each radioisotope may not be simple. Isotopes produced by activation could absorb neutrons and be transmuted into other isotopes. Some activation products may decay into other activation products, increasing the amounts of the latter. Activation products with large neutron absorption cross sections can be burnt out during exposure to neutrons and can change the magnitude of the neutron flux, causing nonlinearity in the neutron transport process. Not all of these factors may need to be considered in calculating the neutron adjoint source of the MS-CADIS method because the importance function needed for speeding up the MC calculation does not require the exact adjoint solution. Additionally, the activated structural materials in fusion energy systems do not typically have large neutron absorption cross sections that can cause either a significant change in the

radioisotope inventory by irradiation of already activated materials or a significant change in the flux. Therefore, the adjoint source defined by Eq. (8) can be reasonably approximated by considering just the major interactions with initial stable isotopes that contribute heavily to the SDDR in fusion energy systems.

The MS-CADIS adjoint neutron source defined in Eq. (8) represents the SDDR resulting from the decay of radioisotopes created through irradiation by a unit neutron flux with energy E_n at location $\vec{r}$. The intuitive response function (adjoint source) for a neutron-only, single-step transport problem is the sum of macroscopic cross sections of the interactions that produce radioisotopes. A related factor in Eq. (8), $m_{ix}(\vec{r})\frac{\sigma_{xi}(E_n)}{\sigma_{xi}(\vec{r})\phi_n^t(\vec{r})}$, represents the microscopic cross section of the radioisotope production reactions multiplied by the mass of each radioisotope existing at the end of the scenario and normalized by dividing it by the interaction rate with one atom. This is proportional to the macroscopic radioisotope production cross section weighted by the fraction of this radioisotope existing at the end of the scenario. The additional weighting function $\int_{E_p} f_i(E_p)\phi_p^+(\vec{r},E_p)dE_p$ represents the importance of each radioisotope produced in region $\vec{r}$ to the final SDDR.

The physical significance of the MS-CADIS adjoint function can be understood by considering the SDDR at the end of the irradiation and decay scenario caused by a unit neutron source at $\vec{r}_0$ and E_0, $q_{n0} = \delta(\vec{r}-\vec{r}_0)\delta(E-E_0)$. The photon source resulting from the irradiation of this unit neutron source can be represented as,

$$q_{p_0} = \left(\sum_i f_i(E_p)\sum_x \left(m_{ix}(\vec{r}) \times \frac{\int_{E_n}\sigma_{xi}(E_n)G_n(\vec{r}_0\rightarrow\vec{r},E_0\rightarrow E_n)dE_n}{\sigma_{xi}(\vec{r})G_n^t(\vec{r}_0\rightarrow\vec{r},E_0)}\right)\right), \tag{10}$$

where $G_n(\vec{r}_0\rightarrow\vec{r},E_0\rightarrow E_n)$ is the Green's function neutron transport kernel and $G_n^t(\vec{r}_0\rightarrow\vec{r},E_0)$ is the neutron transport kernel integrated over neutron energies. By substituting Eq. (10) into Eq. (4), the SDDR caused by irradiation of this unit neutron source can be expressed by,

$$SDDR_0 = \sum_i \left(\int_V \int_{E_p} f_i(E_p)\phi_p^+(\vec{r},E_p)dE_p \times \sum_x m_{ix}(\vec{r}) \frac{\int_{E_n}\sigma_{xi}(E_n)G_n(\vec{r}_0\rightarrow\vec{r},E_0\rightarrow E_n)dE_n}{\sigma_{xi}(\vec{r})G_n^t(\vec{r}_0\rightarrow\vec{r},E_0)} dV \right). \tag{11}$$

To find the MS-CADIS neutron adjoint flux $\phi_{n_0}^+$ resulting from q_{n0}, the MS-CADIS neutron adjoint source defined in Eq. (8) and the neutron flux kernel must be substituted into the neutron adjoint identity represented by the right equality of Eq. (5). It can be easily shown that the MS-CADIS adjoint neutron flux in this case will be equal to $SDDR_0$ in Eq. (11). Therefore, the MS-CADIS adjoint neutron flux represents the contribution of neutrons produced at $\vec{r}_0$ and E_0 to the SDDR that represents the "final" response of the multi-step simulation. It is this physical interpretation that makes the MS-CADIS adjoint neutron flux well suited for accelerating SDDR MC neutron calculations.

2.2 Difference Between MS-CADIS and Global Monte Carlo (MC) Techniques

The use of global MC variance reduction techniques, including Forward Weighted CADIS (FW-CADIS) [12], was suggested for the neutron MC calculations of SDDR analyses [13]. These methods, which attempt to calculate MC tallies with nearly uniform relative uncertainties, will not focus the MC computational efforts on calculating the production rates of radioisotopes that will emit photons which will ultimately contribute to the SDDR. The prohibitive computational costs of these approaches, which increase with the overall problem size and amount of shielding materials, inhibit their ability to accurately predict the SDDR in fusion energy systems using full-scale modeling of an entire fusion plant. Accurate full-scale simulations are required in the design analysis of fusion energy systems such as ITER to determine the effects of important factors such as the cross-talk (interactions) between the different ports on the SDDR behind the ports [2]. The full-scale calculation of the SDDR inside the ITER bioshield will require calculating the neutron fluxes in ~3.8×10^{10} space-energy mesh elements for cubic mesh elements with a side length of 5 cm and 175 energy bins [3].[‡] Even with the unrealistic assumption of using absolutely accurate neutron fluxes for applying global MC variance reduction techniques, the computational cost of an MC calculation that will have non-zero MC scoring in all of these space-energy elements will exceed tens of CPU-years. Contrary to the global MC approach, the MS-CADIS method uses an importance function that represents the importance of the neutrons to the final SDDR or to the final SDDR distribution. This ensures that the computational effort in the MC neutron calculation is focused on the most important parts of the problem.

To illustrate the difference between the MS-CADIS method and global MC methods, the neutron adjoint sources created using the FW-CADIS and MS-CADIS methods for a simple slab shield problem are shown in Fig. 1. The maximum adjoint source strength of the FW-CADIS method is at the extreme corners of the detector side of the steel shield where the forward flux is minimal, while the maximum MS-CADIS adjoint source strength is at the center of the detector side of the steel shield because the activated radioisotopes in this region have the greatest contribution to the SDDR at the detector.

[‡]The FENDL2.1 library [14] that is typically used in fusion application has 175 neutron energy groups.

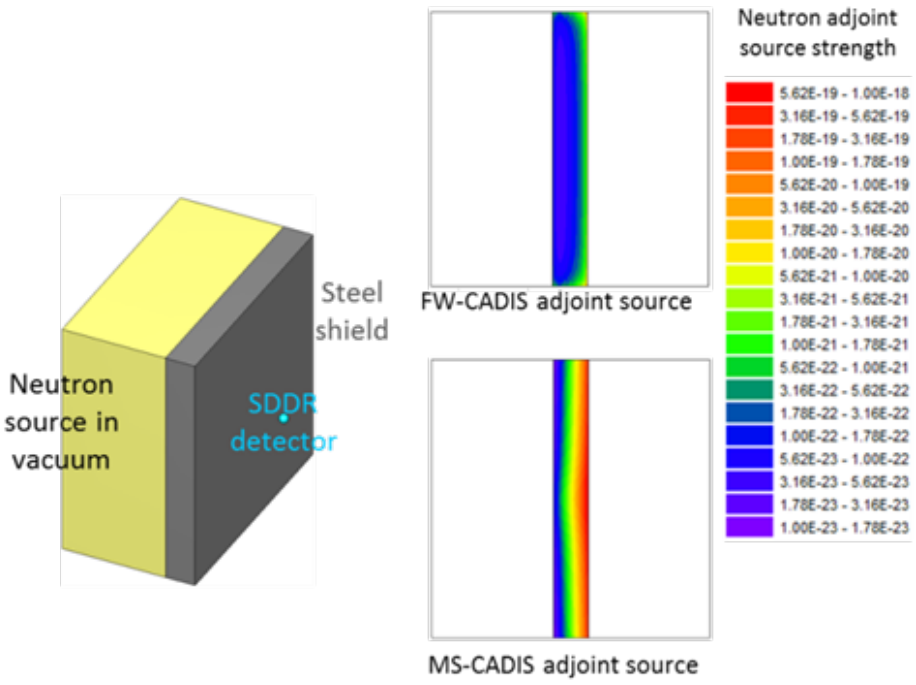

Figure 1. FW-CADIS and MS-CADIS adjoint sources.

2.3 MS-CADIS Implementation

The R2S computational system is based on coupling the activation and MC transport codes and libraries to provide the neutron fluxes calculated from the MC neutron calculation to the activation step and to use the decay photon source in the photon MC calculation. In addition to these calculations, MS-CADIS requires performing (1) a forward deterministic neutron transport calculation to estimate $\sigma_{\mathrm{xi}}(\vec{r})$ and $\phi_n^t(\vec{r})$, (2) activation calculations for each isotope at each element of the deterministic mesh to estimate $m_{ix}(\vec{r})$, (3) an adjoint deterministic photon transport calculation using an adjoint source equal to the flux-to-dose-rate conversion factors at the position of the SDDR detector, and (4) an adjoint deterministic neutron transport calculation with an adjoint source calculated from Eq. (8). Using the CADIS method, the deterministically calculated adjoint neutron and photon fluxes can be used to calculate the source biasing and weight-window parameters to speed up the R2S neutron and photon MC calculations.

Assuming all of the important radioisotopes-producing neutron interactions were accounted for in Eq. (8), the quantity $\frac{m_{ix}(\vec{r})}{\sigma_{xi}(\vec{r})\phi_n^t(\vec{r})}$, which primarily depends on the mass of the initial stable isotope and on the irradiation and decay scenario, should not significantly change with the magnitude and the energy distribution of the neutron flux. The activation calculations in step (2) need to only be repeated few times with different neutron energy distributions to calculate an appropriate value for $\frac{m_{ix}(\vec{r})}{\sigma_{xi}(\vec{r})\phi_n^t(\vec{r})}$ that can be used for calculating the adjoint neutron source at any location $\vec{r}$.

3 TEST PROBLEM

3.1 Problem Description

The simple system shown in Fig. 2 was used to verify the effectiveness of the proposed MS-CADIS method. The system consists of a rectangular parallelepiped of a homogenous mixture of ^{98}Mo and water. The square base of the system had a side length of 150 cm and the height was 250 cm.

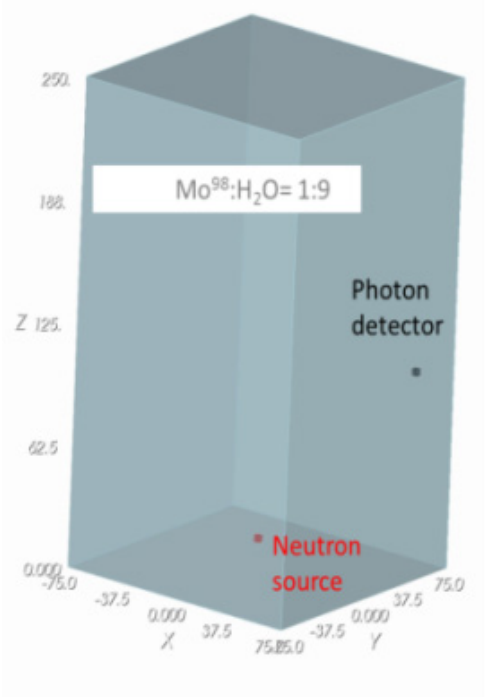

Figure 2. Geometry of simplified example problem.

A monoenergetic (1 MeV) point neutron source with total source strength of 10^{12} neutron/sec was positioned 15 cm above the center of the base. After a very long irradiation time at which the maximum saturation activity of ^{99}Mo was reached, the SDDR was calculated in a cubic volumetric detector with a side length of 2 cm that was placed 60 cm from the source in the *X* and the *Y* directions and 85 cm from the source in the *Z* direction.

3.2 Methodology

Three simplifying assumptions were used for this preliminary test problem: first, only the decay activity caused by neutron absorption of ^{98}Mo was considered and the decay activities from neutron interactions with water constituents and all of the elements of the ^{99}Mo decay chain were ignored; second, only one decay path of ^{99}Mo was considered; finally, the irradiation time was considered to be very long and the cooling time was considered to be very short so that the time dependency of the decay photon production rate could be ignored.

The SCALE6.1 [15] shielding analysis sequence, MAVRIC, was used in this analysis. MAVRIC uses the discrete-ordinates code Denovo for the deterministic calculations and the

multi-group MC code Monaco for the MC calculations [16]. The activation step was not needed in this analysis because of the simplifying assumptions. A 27-neutron-group 19-photon-group ENDF-VII library was used for both the Denovo and the Monaco calculations.

To assess the efficiency and reliability of MS-CADIS, the SDDR values and the Figure of Merit (FOM) of the MC neutron calculation were compared to corresponding values of similar R2S calculations that used the CADIS method to speed up the MC photon calculation and either analog MC or the standard FW-CADIS method for the neutron transport calculation. The use of FW-CADIS as a reference in this analysis provides a reasonable efficiency comparison with other global MC methods because it has been demonstrated that methods such as FW-CADIS that use both forward and adjoint estimates are more efficient in calculating more uniform relative uncertainties across a global mesh tally than other global MC methods that use only forward estimates [17].

3.3 Results

Figure 3 shows the SDDR as a function of the computational time of the Monaco neutron calculations using analog MC, FW-CADIS, and MS-CADIS. To focus on analyzing the neutron Monaco calculation, the CADIS method was used to speed up the photon Monaco calculation for which the running time was set to be long enough so that the uncertainty due to the photon Monaco calculation was always below 0.5% in all of the cases.

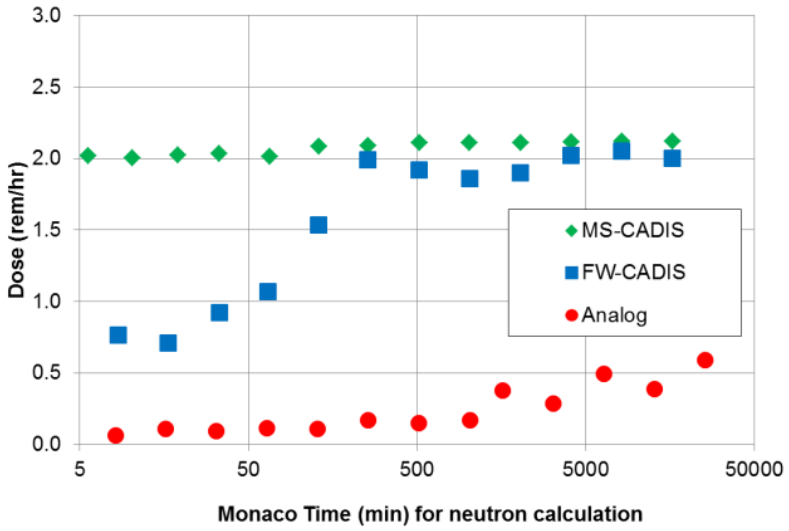

Figure 3. Shutdown dose rates for different run times of neutrons calculations.

MC calculations of responses that are significantly separated from the physical source by strong attenuating shielding materials may be dominated by rare events. These calculations are prone to undersampling problems that can cause inaccurate MC tally estimates. Examining the behavior of the MC estimated mean as a function of number of histories (~time of calculation) is a very effective way of detecting the undersampling problems caused by inadequate sampling of these rare events [18]. A generally monotonically increasing behavior in the calculated SDDR with the time of the analog Monaco neutron calculation was noticed for all of the test cases that

spanned between 8.2 minutes and 17.8 days. Because the difference between the rates of neutron absorption in ^{98}Mo at the source and the detector positions exceeds 11 orders of magnitude and the average simulation time for each neutron in the analog Monaco calculations was ~1 millisecond, it is expected that thousands of days are needed for any reliable answer using analog MC. When the FW-CADIS method was used to accelerate the Monaco neutron calculation, monotonically increasing behavior in the SDDR was noticed with running times of less than 4.3 hours, but the differences in the SDDR of the cases with longer running times did not exceed 10%. With MS-CADIS, the SDDR differences did not exceed 10% for all of the testing cases for which the running times of the neutron Monaco calculation ranged between 5.3 minutes and 11.4 days.

Analyzing the efficiency of the neutron MC calculation requires estimating the uncertainties in the final calculated SDDR due to the uncertainties in the photon source. A new method for propagating uncertainties from the photon source to the final SDDR is currently under development [19]. In this work, the sample standard deviation of multiple SDDR calculations that used neutron Monaco calculations with different random number seeds was used to estimate the uncertainties in the SDDR due to uncertainties in the neutron Monaco calculations. The relative uncertainties and FOMs shown in Table I were calculated using 100 independent replicas of the SDDR calculations that used neutron Monaco calculations with 100 different random number seeds.

Table I. Relative uncertainties and FOMs using MS-CADIS and standard FW-CADIS/CADIS approach

Monaco time (hr)	Relative uncertainty		FOM (1/min)	
	FW-CADIS	MS-CADIS	FW-CADIS	MS-CADIS
4.27	21.56%	0.91%	8.4E-02	47.17
8.53	15.56%	0.66%	8.0E-02	44.84

The mean values of the 100 replicas calculated for each of the FW-CADIS and MS-CADIS cases shown in Table I were ~2.12 rem/hr; the differences between the different methods did not exceed 1σ of the case with the larger uncertainty. These FOMs included neither the small uncertainties due to the photon Monaco calculations nor the running times of either the deterministic calculations or the photon Monaco calculations. If the deterministic run time and the time of the Monaco photon calculations are included in the FOM analysis, the ratio between the efficiency of MS-CADIS to the efficiency of the standard FW-CADIS approach will be ~2% higher than the indicated FOMs ratio because the forward deterministic neutron calculation was not required for MS-CADIS calculations due to the simplifying assumptions in this example problem.

The use of MS-CADIS provided a factor of more than 550 enhancement in the efficiency of the SDDR calculations compared to the standard FW-CADIS/CADIS approach. The uncertainties were not calculated for either the analog Monaco cases or the FW-CADIS cases with shorter running times because the uncertainties in undersampled MC results are meaningless, but the speed up compared to analog MC is expected to be very large (>10,000)

because the SDDR was still undersampled, even when the running times of the analog Monaco neutron calculations were longer than 10 days.

4 CONCLUSIONS

A novel hybrid MC/deterministic technique has been proposed to speed up the MC transport simulations in multi-step shielding analysis such SDDR calculations. Using an importance function that represents the importance of the neutrons to the final SDDR, the MS-CADIS method develops the weight-windows and source biasing parameters for the neutron MC simulations of the SDDR MC calculations. The MS-CADIS method has been tested with a simplified example. The preliminary results showed that the use of MS-CADIS dramatically enhances the efficiency of the SDDR neutron MC calculations compared to the traditional FW-CADIS approach and compared to analog MC.

5 REFERENCES

1. H. Iida, D. Valenza et al., "Radiation shielding for ITER to allow for hands-on maintenance inside cryostat," *J. Nucl. Sci. Technol.*, **Supplement 1**, pp. 235-242 (2000).
2. R. Pampin, R. Juarez et al., "Investigation of Radiation Cross-Talk Effects on Biological Dose Rates in Maintenance Areas Inside the ITER Tokamak," *ANS RPSD 2014 - 18th Topical Meeting of the Radiation Protection & Shielding Division of ANS,* Knoxville, TN, September 14–18, 2014, on CD-ROM, American Nuclear Society, LaGrange Park, IL (2014).
3. A. Ibrahim, P. Wilson et al., "Assessment of Fusion Facility Dose Rate Map Using Mesh Adaptivity Enhancements of Hybrid Monte Carlo/Deterministic Techniques," *Fusion Eng. Des.,* **89** , pp.1875-1879 (2014).
4. M. Youssef, R. Feder, "Summary of the Up-to-Date 3-D Nuclear Analyses of ITER Diagnostics Generic Equatorial Port Plug (GEPP) Performed with the Attila Design Code," *Fusion Sci. Tech.*, **64**, pp. 571-581 (2013).
5. R. Pampin, M. J. Loughlin et al., "Radiation Transport Analyses for Design Optimisation of the ITER Core LIDAR Diagnostic," *Fusion Sci. Tech.*, **56**, pp. 751-755 (2009).
6. Y. Chen, U. Fischer, "Rigorous MCNP Based Shutdown Dose Rate Calculations: Computational Scheme, Verification Calculations and Application to ITER," *Fusion Eng. Des.,* **63,** pp. 107-114 (2002).
7. G. Goertzel, K. Kalos, "Monte Carlo Methods in Transport Problems," *Prog. Nucl. Energy*, **2**, pp. 315-369 (1958).
8. J. C. Wagner, A. Haghighat, "Automated Variance Reduction of Monte Carlo Shielding Calculations Using the Discrete Ordinates Adjoint Function," *Nucl. Sci. Eng.*, **128**, pp. 186-208 (1998).
9. J. C. Wagner, D. E. Peplow, S. W. Mosher, T. M. Evans, "Review of hybrid (deterministic/Monte Carlo) radiation transport methods, codes, and applications at Oak Ridge National Laboratory," *Progress in Nuclear Science and Technology*, **2** , pp. 808-814 (2011).

10. E. E. Lewis, W. F. Miller Jr., *Computational Methods of Neutron Transport, American Nuclear Society*, American Nuclear Society, La Grange Park, IL (1993).

11. D. Vondy, *Development of General Method of Explicit Solution to the Nuclide Chain Equations for Digital Machine Calculations*, Oak Ridge National Laboratory report, ORNL-TM-361, Oak Ridge, TN (1962).

12. J. C. Wagner, D. E. Peplow, S. W. Mosher, "FW-CADIS Method for Global and Regional Variance Reduction of Monte Carlo Radiation Transport Calculations," *Nuc. Sci. Eng.,* **176**, pp. 37-57 (2014).

13. A. Davis, A. Turner, "Application of Novel Global Variance Reduction Methods of Fusion Radiation Transport Problems," *Proc. 2011 Int. Conf. on Advances in Math., Comp. Methods, and Reactor Physics*, Rio de Janeiro, Brazil, May 8–12, 2011, American Nuclear Society, LaGrange Park, IL (2011).

14. D. L. Aldama, A.Trkov, "FENDL2.1, Update of an Evaluated Nuclear Data Library for Fusion Applications," IAEA report INDC (NDS) 467, Vienna, Austria (2004).

15. S. M. Bowman, "SCALE 6: Comprehensive Nuclear Safety Analysis Code System," *Nucl. Techn.,* **174**, pp. 126–148 (2011).

16. D. E. Peplow, "Monte Carlo Shielding Analysis Capabilities with MAVRIC," *Nucl. Tech*., **174**, pp. 289-313 (2011).

17. D. Peplow, "Comparison of Hybrid Methods for Global Variance Reduction in Shielding Calculations," *Proc. 2013 Int. Conf. on Advances in Mathematics, Computational Methods, and Reactor Physics,* Sun Valley, ID, May 5–9, 2013, pp. 231–242 (2013).

18. W. Viera, P. Stevens, "Analysis of the Sampling Distribution in Monte Carlo Radiation Transport Calculations," *Ann. Nucl. Energy*, **22**, pp. 51-55 (1995).

19. D. Peplow, A. Ibrahim, R. Grove, "Propagation of Uncertainty from a Source Computed with Monte Carlo," *Trans. of Am. Nuc. Soc.***, 108**, 643-646 (2013).